EXPERIMENTAL ANALYSIS OF FLUIDIC MUSCLES

FILIP DYRR, LUKAS DVORAK, KAMIL FOJTASEK, PETR BRZEZINA, LUMIR HRUZIK, ADAM BURECEK

VSB – Technical University of Ostrava, Faculty of Mechanical Engineering, Department of Hydromechanics and Hydraulic Equipment, Ostrava, Czech Republic

DOI: 10.17973/MMSJ.2022_10_2022070

filip.dyrr@vsb.cz

Fluidic muscles have been the subject of research since the 1930s to the present day. McKibben's muscle is one of the most common ones. This type is the basis for fluidic muscles already being used commercially. The power-to-weight ratio is one of their main advantages. The disadvantage is difficult handling. The article describes experimental verification of static characteristics of fluidic muscles. During muscle contraction, a tensile force is developed which changes as the length of the muscle changes. This dependence is experimentally verified. A measuring equipment for testing fluidic muscles of various lengths and diameters is designed and assembled. The device consists of a pneumatic circuit, where the output drive is a loaded fluidic muscle. The load of muscle is generated by a hydraulic cylinder. The results will be further applicable to fluidic muscle simulations.

KEYWORDS

fluidic muscle, McKibben muscle, pneumatic artificial muscle, braid angle, static characteristics, experimental equipment

1 INTRODUCTION

The first device that was similar in shape and operation to the human muscle was the invention of the Russian scientist Garasiev. This muscle was designed to drive bioprostheses and was invented in the 1930s [Karnik 1999]. R. C. Pierce, H. De Haven, A. H. Morin can also be included among the first authors of braided artificial muscles. R. H. Gaylord was the first author, who described the force generated by muscle mathematically [Pierce 1936], [De Haven 1949], [Morin 1953], [Gaylord 1958]. In the 1950s, J. L. McKibben invented a version of artificial muscle for limb prostheses. His work was followed by H. F. Schulte, who in 1962 published details of the use of McKibben's muscle together with a mathematical analysis that included Gaylord's patent. [Davis 2003], [Pitel 2015]. Further research progress in the field of artificial muscles occurred, including Nazarczuk's artificial muscle from 1964, the artificial muscle of Prof. Morecki and Baldwin's artificial muscle [Karnik 1999], [Kolibal 2016], [Baldwin 1969]. After that, there was a slowdown in the research of artificial muscles due to the complexity of controlling the equipment, the need for a source of compressed air and also improving the parameters of electric actuators. Further research progress in the field of artificial muscles occurred with the increase of the availability of mathematical modeling and with the progress of control technology [Davis 2003], [Pitel 2015]. Additional artificial muscles were invented. These included ROMAC by G. B. Immega, Rubbertuator by Bridgestone Corporation, simple artificial muscles by Liang and Winters, or muscle by J. N. Marcincin. [Winters 1990], [Karnik 1999], [Kolibal 2016]. Several other companies have been involved in the research, such as Shadow Robot Company, Merlin Systems Corporation or Festo [Pitel 2015].

Caldwell, Tsagarakis and others have addressed the issue of artificial muscles in their publications. The authors have written several publications that deal with artificial muscle, its management and use in various applications [Caldwell 1995], [Focchi 2010]. Fluidic muscle is also well described in publications by Daerden and Lefeber. The authors divided artificial muscles based on their connection [Daerden 2002]. Tondu, Lopez also have addressed the issue of artificial muscles. One of the publications deals with the use of these actuators in robotics. The publication also deals with the force dependence of muscle contraction [Tondu 2000]. Sarosi compared different fluidic muscles in his publication, comparing the force dependencies of muscle contraction. [Sarosi 2016] Pitel, Hrosovsky et al. wrote a publication in 2015 that deals with artificial muscles. The book includes modeling, simulation and control [Pitel 2015]. Many types of artificial muscle have been designed and studied. However, the most widely used type of artificial muscle is McKibben's braided muscle design. Festo has invented a fluidic muscle that is based on the McKiben muscle. The difference is the integration of the aramid fibers of braid directly into the rubber muscle tube. This modification reduces the problems associated with friction between the tube and the braid, and overall, the muscle design is more robust and durable. The muscle is used in robotics and industrial applications, for example as an actuator in clamping, vibrating or lifting devices. [Festo 2022].

These fluidic muscles are used for experimental analysis. The article compares the force dependencies of muscle contraction for fluidic muscles with different diameter and length. Furthermore, the detailed geometric dimensions for one fluidic muscle are determined. These dimensions are used for the analytical calculation of the theoretical force generated by the muscle. A simple static physical model is chosen for the analytical calculation, which is based on general muscle parameters and does not take into account losses due to friction, rubber deformation, influence of end caps etc. The analytical calculation obtains the theoretical force dependence of muscle contraction. The result is a comparison of measured data and analytical calculation.

2 MATHEMATICAL DESCRIPTION

Mathematical modeling is a good way to obtain valuable data in the design or control phase of a fluidic muscle. Mathematical simulation of devices with fluidic muscle will make it possible to obtain, for example, the course of the dynamic behaviour of the entire system. To rightly define a mathematical model, it is neccesary to know the geometric properties of the muscle and the physical phenomenas that occur in the muscle during its operation. Significant problems in fluidic muscle modeling include friction between the braid fibers and the rubber tube, flexibility of construction, the effect of end caps, and more. For these reasons, it is not possible to create a perfectly accurate mathematical model. Fluidic muscle is a nonlinear element with a range of insensitivity and hysteresis. Several mathematical models have been made. Mathematical models can be divided into several categories. The first group consists of empirical models (Gavrilovic a Maric, 1969, Medrano-Cerda et al., 1995). Another group is based on muscle geometry (Gaylord, 1958, Schulte 1961, Tondu et al., 1994, Paynter, 1996). The following group is based on material properties (Chou, 1996, Schulte, 1961, Huxley, 1957). The last group consists of phenomenological and biomechanical models (Hill 1938) [Pitel 2015].

The geometric model describes a muscle in terms of its geometric properties. With certain simplifications, static characteristics of fluidic muscles can be obtained. One way of mathematical description is to model a fluidic muscle as a cylinder with zero wall thickness. In this case, the main parameters are the initial radius of the muscle r_0, initial length l_0 and initial braid angle relative to the longitudinal axis of the muscle α_0 e.g. see Fig. 1 [Pitel 2015].

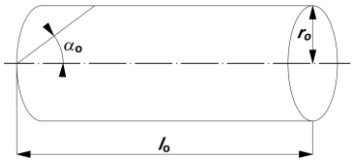

Figure 1. Main parameters for a simple geometric model of an artificial muscle

According to the law of conservation of energy, there is an equality between the input work dW_{in}, performed by the compressed air supplied to the muscle and the output work dW_{out}, performed by the muscle by its contraction [Chou 1996], [Pitel 2015]:

$$dW_{in} = dW_{out}. \tag{1}$$

The input work dW_{in} is done in the muscle when gas pushes the inner bladder surface e.g. see Fig. 2. This is [Chou 1996], [Pitel 2015]:

$$dW_{in} = \int_S (p' - p_0) \cdot dl \cdot dS = p \cdot dV, \tag{2}$$

where p' is absolute air pressure in the muscle, p_0 is atmospheric pressure, p is working pressure in the muscle, S is the total internal area of the muscle and dV is a change in muscle volume.

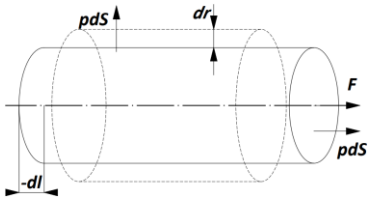

Figure 2. The relationship between air pressure and muscle contraction for output work dW_{out}

The output work dW_{out} is done when the actuator shortens associated with the volume change, which is [Chou 1996], [Pitel 2015]:

$$dW_{out} = -F \cdot dl, \tag{3}$$

where F is the axial tension, and dl is the axial displacement. Substituting equation (2) and (3) into equation (1), we obtain the expression of the tensile force of muscle F on the relative pressure p in muscle [Chou 1996], [Pitel 2015]:

$$F = -p \cdot \frac{dV}{dl}. \tag{4}$$

The elongation of the braid when applying pressure to the muscle is very small, and therefore we consider only the dependence on its length b. For the following equations we use the mentioned constant fiber length b, the initial muscle length l_0 and the number of turns N of one fiber around the longitudinal axis of the muscle, e.g. see Fig. 3 [Chou 1996], [Pitel 2015].

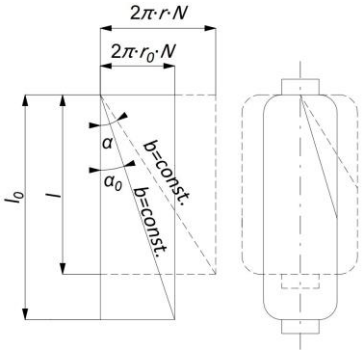

Figure 3. The dependence between the parameters of a simple geometric muscle model

The length of the muscle l and its radius r can be expressed as a function of the braid angle α with a constant parameter N, which represents the number of turns of the braid, and a constant parameter b, which represents the length of the braid [Chou 1996], [Pitel 2015]:

$$l = b \cdot cos\alpha, \tag{5}$$

$$r = \frac{b \cdot sin\alpha}{2\pi \cdot N}. \tag{6}$$

Assuming zero cylinder wall thickness, using equations (5) and (6) and subsequent adjustment, we obtain the cylinder volume V [Chou 1996], [Pitel 2015]:

$$V = \pi \cdot r^2 \cdot l = \frac{b^3}{4\pi \cdot N^2} \cdot sin^2\alpha \cdot cos\alpha. \tag{7}$$

Substituting equation (7) into equation (4) for the tensile force F of the muscle we obtain [Chou 1996], [Pitel 2015]:

$$F = -p \cdot \frac{\frac{dV}{d\alpha}}{\frac{dl}{d\alpha}} = -p \cdot \frac{\frac{b^3}{4\pi \cdot N^2} \cdot (2sin\alpha \cdot cos^2\alpha - sin^3\alpha)}{-b \cdot sin\alpha} = \tag{8}$$

$$= p \cdot \frac{b^3 \cdot sin\alpha \cdot (2cos^2\alpha - sin^2\alpha)}{4\pi \cdot N^2 \cdot b \cdot sin\alpha} = p \cdot \frac{b^2 \cdot (3cos^2\alpha - 1)}{4\pi \cdot N^2}.$$

Equation (8) shows that the tensile force F of a muscle is directly proportional to the pressure of the compressed air and is a function of the braid angle. Substituting for $cos\ \alpha$ equation (5) we obtain the tensile force F dependence of the length of the muscle l [Chou 1996], [Pitel 2015]:

$$F = p \cdot \frac{3l^2 - b^2}{4\pi \cdot N^2}. \tag{9}$$

The change in muscle length can be expressed as a contraction κ, or the ratio of muscle contraction to the initial muscle length l_0 [Chou 1996], [Pitel 2015]:

$$\kappa = \frac{l_0 - l}{l_0}, \tag{10}$$

Thus, it is possible to express the dependence of the tensile force F on the contraction κ [Chou 1996], [Pitel 2015]:

$$F = p \cdot \frac{3l_0^2 \cdot (1 - \kappa)^2 - b^2}{4\pi \cdot N^2}, \tag{11}$$

which is equivalent to [Chou 1996]:

$$F = \frac{\pi \cdot D_M^2 \cdot p}{4} \cdot (3cos^2\alpha - 1), \tag{12}$$

where D_M is maximal theoretical diameter when the braid angle $\alpha = 90°$, which is the same form used in Schulte´s paper. The maximal shortening will be reached when $F = 0$ N, that is, braid angle $\alpha = 54{,}7$ ° [Chou 1996].

The mentioned geometric model based on the main parameters of the fluidic muscle, where the input work

is converted into the theoretical force of the muscle F_t, has several properties [Tondu 2000].

Theoretical tensile force of the muscle F_t

- is proportional to muscle cross-sectional area,
- is independent of the initial length l_0,
- is proportional to control pressure p,
- increases as the muscle initial braid angle α_0 decreases,
- decreases almost linearly with contraction ratio according to a slope proportional to control pressure p.

3 GEOMETRY

One of the main part of this paper is an experimental measurement the tensile force F dependence of the contraction κ. Fluidic muscles of different diameters and lengths were used for measurement e.g. see Tab. 1.

muscle	nominal diameter	length
DMSP 20-250	20 mm	250 mm
DMSP 20-500	20 mm	500 mm
DMSP 10-250	10 mm	250 mm
DMSP 10-500	10 mm	500 mm

Table 1. Measured fluidic muscles

Fluidic muscle DMSP20-250 was prepared to measure detailed geometric dimensions, including initial braid angle α_0. After removing the part of rubber tube, it was possible to measure the initial braid angle, which is made from aramid fibers. Knowledge of the braid angle α_0 in the unloaded state is necessary to determine the theoretical tensile force F_t dependence of the contraction κ. Furthermore, the wall thickness t, the unstretched braid length b, the number of turns of the braid around the longitudinal axis of the muscle N are measured e.g. see Tab. 2.

DMSP20 – 250 geometry		
Inner diameter d_{in}	19,5	mm
Outer diameter d_{out}	23,5	mm
Wall thickness t	2	mm
Initial length l_0	250	mm
Initial braid angle α_0	25	°
Number of braids n	2	
Unstretched braid length b	275,85	mm
Number of turns per braid N	1,73	

Table 2. Geometry of DMSP20-250

The obtained values are used to create a simple geometric model and analytical determination of the theoretical tensile force F_t dependence of the contraction κ. It can be seen from the detailed photographs that the braid is fully integrated into the rubber tube, which results in reduced friction between the rubber and the braid. Overall, the construction is more robust and much more durable for industrial use e.g. see Fig. 4.

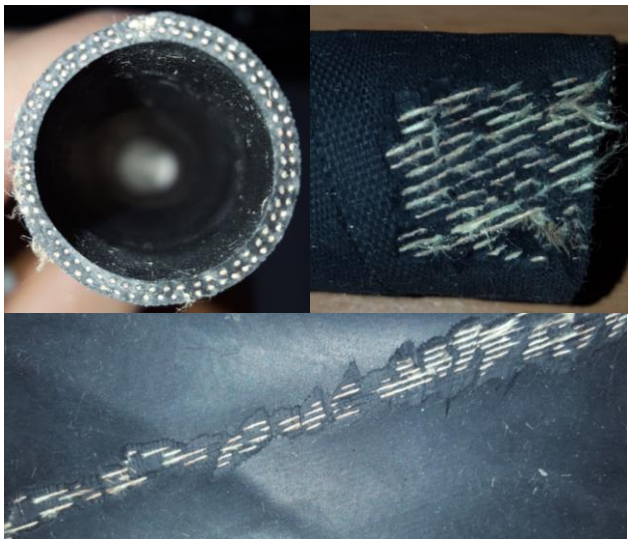

Figure 4. Geometry of DMSP20 by Festo

4 EXPERIMENTAL EQUIPMENT

The experimental equipment for measuring fluidic muscles of different diameters and lengths was created for research in the field of fluidic muscles. The construction is made of modular aluminium profiles for easy modification. The tested fluidic muscle FM is connected to the plate, which is attached to the top of the construction. The working air pressure in muscle p is set to the required value by the pressure reducing valve RV_M. The working air pressure p is measured by a pressure sensor PS. When filling the muscle FM with compressed air, the length l of the muscle FM changes, which is measured by the distance laser sensor DLS. As the working air pressure p increases, the tensile force F of the muscle FM increases, which is measured by the force sensor FS. The force sensor FS is located between the lower end cap of the fluidic muscle FM and the piston rod of the hydraulic cylinder HC, which generates the load of the fluidic muscle FM. The movement of the hydraulic cylinder HC is controlled by a 4/3 directional valve DV_{HC}. The working pressure of the oil p_{HC} in the hydraulic cylinder HC is set to the required value by the relief valve RV_{HC}. The relief valve RV_{HC} is parallel connected at the piston rod side of the hydraulic cylinder HC. Increasing the working pressure of the oil p_{HC} increases the load on the fluidic muscle FM e.g. see Fig. 5, 6.

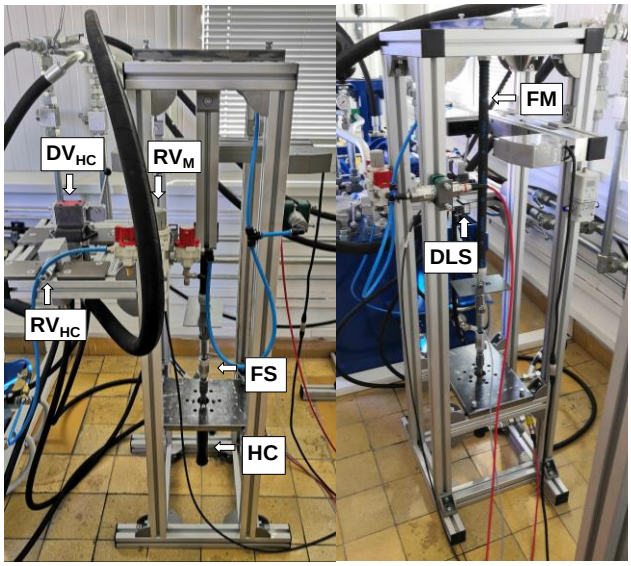

Figure 5. Experimental equipment for measuring of fluidic muscles

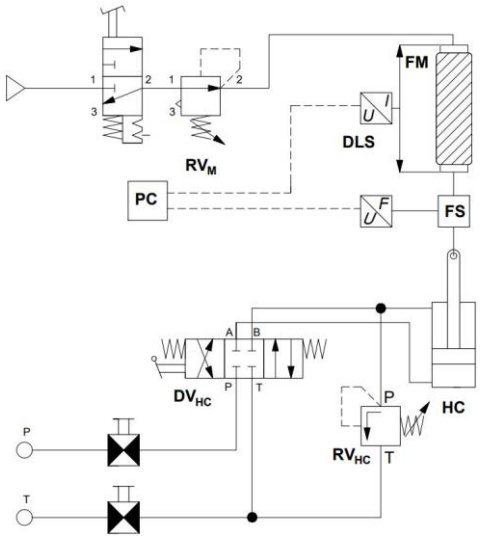

Figure 6. Scheme of experimental equipment for measuring of fluidic muscles

5 MEASUREMENT

Fig. 7 shows the force F dependence of the muscle contraction κ at pressures p = (100 ÷ 600) kPa for fluidic muscles DMSP20. The Graph lists comparison of measured dependencies and dependencies, which are specified by the Festo catalog. Fluidic muscle DMSP20 with length l = 250 mm and 500 mm was measured. The graph lists that measured dependencies for both lengths have the same trend at each working pressure p. The measured dependencies have the same trend as the dependence from the Festo catalog at the pressure p = 100 kPa. The measured force F is lower than the force from the Festo catalog across the entire contraction range at the pressure p = (200 ÷ 600) kPa.

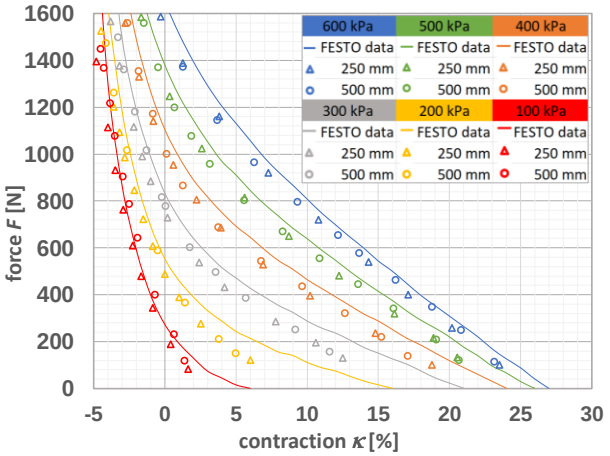

Figure 7. Comparison between force F dependencies of contraction κ for muscles DMSP20

Fig. 8 shows the force F dependence of the muscle contraction κ at pressures p = (100 ÷ 600) kPa for fluidic muscles DMSP10. The Graph lists comparison of measured dependencies and dependencies, which are specified by the Festo catalog. Fluidic muscle DMSP10 with length l = 250 mm and 500 mm was measured. The graph lists that measured dependencies for both lengths have the same trend at working pressure p = (100 ÷ 500) kPa. The measured force F of the muscle with length l = 500 mm is higher at the pressure p = 600 kPa. During the shortening the measured force F of the muscle with both lengths l is lower than the force from the Festo catalog at the pressure p = (100 ÷ 600) kPa. During the elongation of the muscle, the measured trend of the force F has a better match with the trend of the force F from the Festo catalog at each working pressure p.

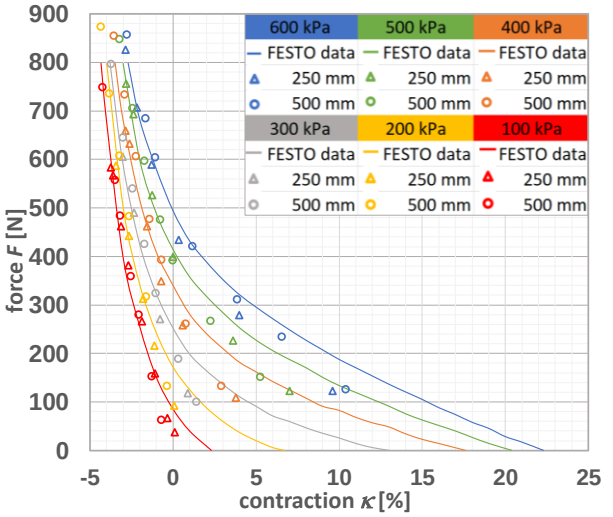

Figure 8. Comparison of the force F dependencies of contraction κ for muscles DMSP10

Fig. 9 shows a comparison between the analytical calculation of the theoretical tensile force F_t depending on the contraction κ at different working pressures according to equation 11 with the measured dependencies for the fluidic muscle DMSP20 with length l = 250 mm, for which have determined the necessary geometric parameters. The static geometric model used for the analytical calculation is a simple model based on the geometric parameters of the muscle. It does not take into account the losses that actually occur in the muscle. These are passive resistances formed by friction of the braid fibers with rubber, deformation of rubber, the effect of end caps and more. This simple model transforms all input work into theoretical tensile force F_t. The measured values correspond to the real state, where part of the input work is absorbed by losses. The graph lists that at contraction κ = (0 ÷ 25) %, when the muscle shortens, the actual tensile force F is less than the analytically calculated force F_t at each working pressures p. Graph lists that the analytical determined force F_t is lower than measured force F at constant working pressure during the contraction $\kappa \leq$ (-2 ÷ -0.6) % (depending on the working pressure p). This is due to the material and geometric properties of the muscle during its elongation, when the muscle is stretched by an external force.

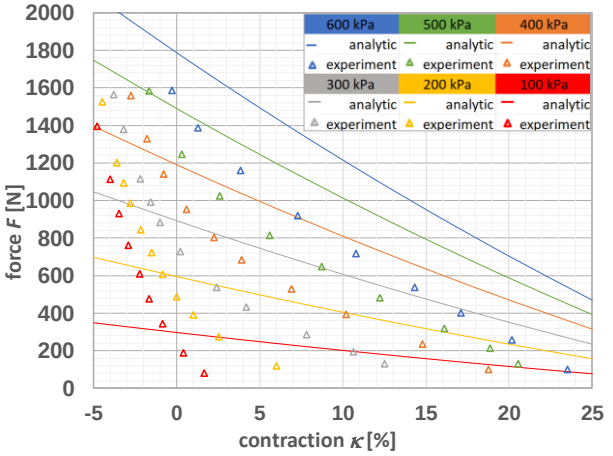

Figure 9. Comparison between the theoretical force F_t and the actual force F dependencies of the contraction κ for the DMSP20 muscle with length l = 250 mm

Fig. 10 shows the muscle efficiency η dependence of the contraction κ, which is determined according to the equation (13):

$$\eta = \frac{F}{F_t}. \tag{13}$$

The efficiencies are determined only during the shortening based on the above comparison, see Fig. 9. The graph lists that the efficiency η decreases with increasing contraction κ at each working pressure p.

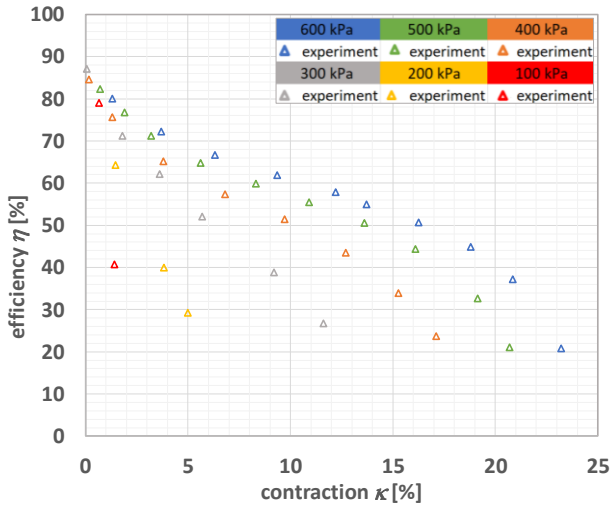

Figure 10. The efficiency η dependencies of contraction κ for muscle DMSP20 with length l = 250 mm

6 CONCLUSIONS

The measuring equipment for testing fluidic muscles of various lengths and diameters was designed and assembled. The tensile force dependence of the contraction was measured for fluidic muscles of different lengths and diameters. The measured dependencies of tensile force on contraction were compared with the dependencies reported by the Festo catalog. Geometric parameters were determined for the selected fluidic muscle for the analytical calculation of the theoretical tensile force dependence of the contraction. The theoretical tensile force dependencies of the contraction were compared with the measured dependencies.

ACKNOWLEDGMENTS

This work was supported by the European Regional Development Fund in the Research Centre of Advanced Mechatronic Systems project, project number CZ.02.1.01/0.0/0.0/16_019/0000867 within the Operational Programme Research, Development and Education.

The work presented in this paper was supported by a grant SGS „Numerical modeling of transient fluid flow problems with the support of experimental research." SP2022/32.

CONTACTS:

Ing. Filip Dyrr
Department of Hydromechanics and Hydraulic Equipment,
Faculty of Mechanical Engineering,
VSB – Technical University of Ostrava
17. listopadu 15, Ostrava – Poruba, 708 33, Czech Republic
+420 596 994 492, filip.dyrr@vsb.cz

REFERENCES

[Baldwin 1969] Baldwin, H.A. Realizable Models of Muscle Function. In Biomechanics, Proceedings of First Biomechanics Symposium, Plenum Press, New York, 1969, pp. 139-148.

[Caldwell 1995] Caldwell, D.G. et al. Control of Pneumatic Muscle Actuators, IEEE Control Systems Magazine, vol. 15, number 1, 1995, pp. 40-48. 1995.

[Chou 1996] Chou, C., Hannaford, B. Measurement and Modeling of McKibben Pneumatic Muscles. IEEE Transactions on Robotics and Automation, 1996, vol. 12, no. 1, pp. 90-102.

[Daerden 2002] Daerden, F, Lefeber, D. Pneumatic Artificial Muscles: Actuator for Robotics and Automation. European Journal of Mechanical and Environmental Engineering, Vol. 47, No. 1, pp. 11-21.

[Davis 2003] Davis, S. et al. Enhanced Modelling and Performance in Braided Pneumatic Muscle Actuators. International Journal of Robotic Research, 2003, Vol.22, No.3-4, pp 213-228.

[De Haven 1949] De Haven, H. Tensioning Device for a Producing a Linear Pull Cover. U.S. Patent 2,483,088, 27 September 1949.

[Festo 2022] Fluidic Muscle DMSP. Festo product catalog. [online] [20. 02. 2022]. Available from: https://www.festo.com/media/pim/555/D15000100140555.PDF

[Focchi 2010] Focchi, M. et al. Water/Air Performance Analysis of a Fluidic Muscle. IEEE/RSJ International Conference on Intelligent Robots and Systems, Taipei, 2010, pp. 2194-2199.

[Gaylord 1958] Gaylord, R.H. Fluid Actuated Motor System and Stroking Device. U.S. Patent 2,844,126, 22 July 1958.

[Karnik 1999] Karnik, L., Novak Marcincin, J. Biorobotic Equipment. Opava: Marfy Slezsko, 1999. ISBN 80-902746-0-9 (in Czech).

[Kolibal 2016] Kolibal, Z. Robots and Robotic Manufacturing Technologies. Brno: Vutium, 2016. ISBN 978-80-214-4828-5 (in Czech).

[Morin 1953] Morin, A.H. Elastic Diaphragm. U.S. Patent 2,642,091, 16 June 1953.

[Pierce 1936] Pierce, R.C. Expansible Cover. U.S. Patent 2,041,950, 26 May 1936.

[Pitel 2015] Pitel, J. et al. Pneumatic Artificial Muscles: Modelling, Simulation, Control. Kosice: Technical University of Košice, 2015. ISBN 978-80-553-2164-6 (in Slovak).

[Tondu 2000] Tondu, L., Lopez, P. Modeling and Control of McKibben Artificial Muscle. IEEE Control System Magazine, 2000, pp. 15-38.

[Sarosi 2016] Sarosi, J., Comparison of Different Fluidic Muscles, The 9th International Symposium about Machine and Industrial Design in Mechanical Engi-neering (KOD 2016), Balatonfured, 2016, pp. 147-150.

[Winters 1990] Winters, J.M. Braided Artificial Muscles: Mechanical Properties and Future Uses in Prosthetics and Orthotics. Resna 13th Annual Conference, Washington D.C., 1990, pp. 173-174.